

Weak Galerkin finite element method for second order problems on curvilinear polytopal meshes with Lipschitz continuous edges or faces

Qingguang Guan

School of Mathematics and Natural Sciences, University of Southern Mississippi, Hattiesburg, MS 39406, USA

Gillian Queisser

Department of Mathematics, Temple University, Philadelphia, PA 19122, USA

Wenju Zhao*

School of Mathematics, Shandong University, Jinan, Shandong 250100, China

Abstract

In this paper, we propose new basis functions defined on curved sides or faces of curvilinear elements (polygons or polyhedrons with curved sides or faces) for the weak Galerkin finite element method. Those basis functions are constructed by collecting linearly independent traces of polynomials on the curved sides/faces. We then analyze the modified weak Galerkin method for the elliptic equation and the interface problem on curvilinear polytopal meshes with Lipschitz continuous edges or faces. The method is designed to deal with less smooth complex boundaries or interfaces. Optimal convergence rates for H^1 and L^2 errors are obtained, and arbitrary high orders can be achieved for sufficiently smooth solutions. The numerical algorithm is discussed and tests are provided to verify theoretical findings.

Keywords: Lipschitz Continuous Boundaries or Interfaces; Curvilinear Elements; Weak Galerkin Method; Traces of Polynomials; High Orders; Second-Order PDEs

2010 MSC: 65N30, 65N12, 35J25

1. Introduction

It has been a challenging question: how to design high-order numerical methods solving Partial Differential Equations (PDEs) on domains (2D or 3D) with less smooth curved boundaries or interfaces if the solutions are sufficiently smooth? We refer [1, 2, 3, 4, 5] for high-order methods with piecewise C^2 boundaries or interfaces, and [6, 7] for high-order methods relying on the smoothness of the boundaries/interfaces. Many numerical methods fall within those two categories. Our approach based on the weak Galerkin finite element method only needs boundaries or interfaces to be Lipschitz continuous, and the convergence rates depend on the solution, not the geometry. The weak Galerkin method [8, 9, 10, 11] among others (e.g., HDG [12, 4], nonconforming VEM [13, 14], HHO[15, 16]) as a new variation of Galerkin methods has been applied to various partial differential equations [9, 17, 18, 19]. The main advantages of those methods lie in using discontinuous basis functions inside the element and on its boundaries, employing general shape elements, ensuring mass conservation, and producing continuous numerical fluxes. HDG, HHO, VEM, and other methods with curved elements dealing with elliptic interface problems and Dirichlet boundary value problems can be found in [12, 4, 15, 16, 7, 20] and references therein. The method proposed here is significantly different from them, it uses fitted meshes, and there is no need to map to reference elements and redefine basis functions. An early version of this paper in 2019, without numerical experiments, can be found

*Corresponding author

Email addresses: qingguang.guan@usm.edu (Qingguang Guan), gillian.queisser@temple.edu (Gillian Queisser), zhaowj@sdu.edu.cn (Wenju Zhao)

on **arXiv**, see [21]. Similar idea was also introduced in the Virtual Element context for 2D problems, see [22]. Later development by other researchers includes [17, 23, 24, 25], but our method is still unique with relaxed requirements for regularities of boundaries/interfaces and uniform treatment in 2D and 3D. The key idea of the weak Galerkin finite element method is the definition of “weak gradient”. Suppose we have a curvilinear polygonal or polyhedral domain $D \subset \mathbb{R}^n$, ($n = 2, 3$) with interior part D_0 and $C^{0,1}$ boundary ∂D , see Figure 1 for a 2D example. A discontinuous function $v = (v_0, v_b)$ on D is defined as: $v_0 \in L^2(D_0)$, $v_b \in L^2(\partial D)$. Then we denote $W(D)$ as the space of those discontinuous functions

$$W(D) = \{v = (v_0, v_b) : v_0 \in L^2(D_0), v_b \in L^2(\partial D)\}. \quad (1)$$

For any $v \in W(D)$, the “weak gradient” of v is a linear functional in the dual space of $[H^1(D)]^n$, it’s defined by $\nabla_w v$ in (2)

$$(\nabla_w v, \vec{q})_D := - \int_D v_0 \nabla \cdot \vec{q} \, dx + \int_{\partial D} v_b \vec{q} \cdot \vec{n} \, dS, \quad \forall \vec{q} \in [H^1(D)]^n, \quad (2)$$

where \vec{n} is the outward normal vector to ∂D . The discrete “weak gradient” $\nabla_{w,k,D} v$ of $v \in W(D)$ is defined as the solution of equation (3)

$$(\nabla_{w,k,D} v, \vec{q})_D = - \int_D v_0 \nabla \cdot \vec{q} \, dx + \int_{\partial D} v_b \vec{q} \cdot \vec{n} \, dS, \quad \forall \vec{q} \in [\mathbb{P}_k(D)]^n, \quad (3)$$

where $\nabla_{w,k,D} v \in [\mathbb{P}_k(D)]^n$, $\mathbb{P}_k(D)$ is the polynomial space with degree no more than k , where k is a non-negative integer. For brevity, in following sections, we use ∇_w to represent $\nabla_{w,k,D}$.

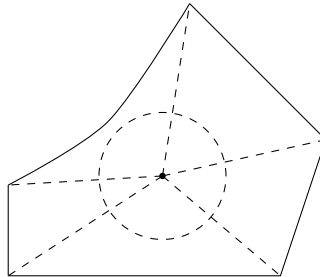


Figure 1: A star-shaped curvilinear element D with a $C^{0,1}$ curved side

The paper is structured as follows. In Section 2, the shape-regular assumptions for curvilinear elements are given, and new L^2 projections on curved sides/faces are defined. Based on the assumptions and projections, necessary lemmas are proved. Then the weak Galerkin finite element scheme and new basis functions are proposed. Section 3 is devoted to solving Poisson’s equation. The newly defined basis functions are used to solve the equation on curvilinear polytopal meshes with Lipschitz continuous edges or faces, where optimal convergence rates in L^2 and H^1 norms are proved. In Section 4, we apply the proposed weak Galerkin method to solve the elliptic interface problem, which involves Lipschitz continuous curved interfaces/boundaries. We also provide an error analysis that demonstrates optimal convergence rates. Section 5 shows the numerical results in 2D. Problems in 3D can be solved similarly but not presented here. Poisson’s equation with the Neumann boundary condition on the curved domain is also considered. The elliptic interface problem with the non-homogeneous jump condition on the interface is tested. For convenience, Lipschitz continuous curved sides on an element are constructed by connecting short lines, but the basis functions are defined on the whole curve. The convergence results for P_1 and P_2 elements are all optimal. Conclusions are drawn in Section 6.

2. Shape regularity

The shape regular assumptions are similar to [26, 19]. Assume

(A1) D is a $C^{0,1}$ curvilinear polygonal/polyhedral domain with diameter h_D ,

(A2) D is star-shaped with respect to a disc/ball $\mathfrak{B}_D \subset D$ with radius $\rho_D h_D$, $0 < \rho_D < \frac{1}{2}$,

(A3) ρ_D has a uniform lower bound $0 < \rho_{\min} < \rho_D$.

Figure 1 is a $C^{0,1}$ curvilinear polygonal domain, which has a Lipschitz continuous curved side. Let $A \lesssim B$ denote $A \leq (\text{constant})B$. D is shape-regular if it satisfies (A1)-(A3). The following Lemmas in Section 2 are valid on such D , and the hidden constants only depend on ρ_D and degrees of employed polynomials.

Lemma 2.1. (Bramble-Hilbert Estimates) [27]. D is shape-regular implies that:

$$\inf_{q \in \mathbb{P}_l(D)} |\xi - q|_{H^m(D)} \lesssim h^{l+1-m} |\xi|_{H^{l+1}(D)}, \quad \forall \xi \in H^{l+1}(D), \quad l = 0, \dots, k, \quad \text{and } 0 \leq m \leq l.$$

Lemma 2.2. (Trace Inequality (2.18)) [26]. If D is shape-regular, then we have

$$h_D^{-1} \|\xi\|_{L^2(\partial D)}^2 \lesssim h_D^{-2} \|\xi\|_{L^2(D)}^2 + \|\nabla \xi\|_{L^2(D)}^2, \quad \forall \xi \in H^1(D).$$

Remark 1. (2.18) in [26] is also valid for D here with curved sides/faces. The proof is the same.

2.1. L^2 Projection Operators

We define the projection Q_h as

$$Q_h v|_D := (Q_{k,D}^0 v_0, Q_{k,D}^b v_b), \quad \forall v \in W(D), \quad (4)$$

where $Q_{k,D}^0$ is the L^2 projection operator from $L^2(D)$ to $\mathbb{P}_k(D)$; $Q_{k,D}^b$ is the L^2 projection operator from $L^2(e)$ to $\mathbb{P}_k|_e$, where e is a side or face of D , no need to be straight or flat, and $\mathbb{P}_k|_e$ is the space of restricted parts of polynomials with degrees no more than k on e .

Then, let $\mathbb{Q}_{k-1,D}$ be the L^2 projection operator from $[L^2(D)]^n$ to $[\mathbb{P}_{k-1}(D)]^n$, $n = 2, 3$.

With shape-regular D and definitions of Q_h and $\mathbb{Q}_{k-1,D}$, we obtain Lemmas 2.3 to 2.6. The proof of Lemma 2.3 can be found in [26] (see Lemma 2.3 and Lemma 3.9). Proofs of Lemmas 2.4 and 2.5 (Lemma 2.5 depends on Lemma 2.1 and (6)) are similar to Lemmas 3 and 6 in [19], respectively. Lemma 2.6 is crucial for the error analysis of our method.

Lemma 2.3. [26] Assume that D is shape-regular. Then, we have

$$|p|_{H^1(D)} \lesssim h_D^{-1} \|p\|_{L^2(D)}, \quad \forall p \in \mathbb{P}_k(D) \quad (5)$$

$$|Q_{k,D}^0 \xi|_{H^1(D)} \lesssim |\xi|_{H^1(D)}, \quad \forall \xi \in H^1(D) \quad (6)$$

Lemma 2.4. [19] For any $\vec{q} \in [\mathbb{P}_k(D)]^n$, D is shape-regular, we have

$$h_D \|\vec{q}\|_{L^2(\partial D)}^2 + h_D^2 \|\nabla \cdot \vec{q}\|_{L^2(D)}^2 \lesssim \|\vec{q}\|_{L^2(D)}^2.$$

Lemma 2.5. [19] Let D be shape-regular, then for $\xi \in H^{k+1}(D)$, we have

$$\|\xi - Q_{k,D}^0 \xi\|_{L^2(D)}^2 + h_D^2 |\xi - Q_{k,D}^0 \xi|_{H^1(D)}^2 \lesssim h_D^{2(k+1)} \|\xi\|_{H^{k+1}(D)}^2, \quad (7)$$

$$\|\nabla \xi - \mathbb{Q}_{k-1,D} \nabla \xi\|_{L^2(D)}^2 + h_D^2 |\nabla \xi - \mathbb{Q}_{k-1,D} \nabla \xi|_{H^1(D)}^2 \lesssim h_D^{2k} \|\xi\|_{H^{k+1}(D)}^2. \quad (8)$$

Lemma 2.6. Let Q_h be the operator in (4). Then with shape-regular D , we have

$$(\nabla_w Q_h \xi, \vec{q})_D = (\mathbb{Q}_{k-1,D} \nabla \xi, \vec{q})_D + \langle Q_{k,D}^b \xi - \xi, \vec{q} \cdot \vec{n} \rangle_{\partial D}, \quad \forall \xi \in H^1(D), \quad (9)$$

$$|\langle Q_{k,D}^b \xi - \xi, \vec{q} \cdot \vec{n} \rangle_{\partial D}| \lesssim h_D^k \|\xi\|_{H^{k+1}(D)} \|\vec{q}\|_{L^2(D)}, \quad \forall \xi \in H^{k+1}(D), \quad (10)$$

$$\|\nabla_w Q_h \xi - \mathbb{Q}_{k-1,D} \nabla \xi\|_{L^2(D)} \lesssim h_D^k \|\xi\|_{H^{k+1}(D)}, \quad \forall \xi \in H^{k+1}(D), \quad (11)$$

where $\vec{q}, \nabla_w Q_h \xi \in [\mathbb{P}_{k-1}(D)]^n$, the hidden constants only depend on ρ_D and k .

Proof. By (3), integration by parts and the definitions of $\mathbb{Q}_{k-1,D}$, Q_h , we have

$$\begin{aligned} (\nabla_w Q_h \xi, \vec{q})_D &= -(Q_{k,D}^0 \xi, \nabla \cdot \vec{q})_D + \langle Q_{k,D}^b \xi, \vec{q} \cdot \vec{n} \rangle_{\partial D} \\ &= -(\xi, \nabla \cdot \vec{q})_D + \langle \xi, \vec{q} \cdot \vec{n} \rangle_{\partial D} + \langle Q_{k,D}^b \xi - \xi, \vec{q} \cdot \vec{n} \rangle_{\partial D} \\ &= (\mathbb{Q}_{k-1,D} \nabla \xi, \vec{q})_D + \langle Q_{k,D}^b \xi - \xi, \vec{q} \cdot \vec{n} \rangle_{\partial D} \end{aligned}$$

so that (9) is obtained.

To get (10), with Lemma 2.4, we have

$$\begin{aligned} |\langle Q_{k,D}^b \xi - \xi, \vec{q} \cdot \vec{n} \rangle_{\partial D}| &\lesssim \|Q_{k,D}^b \xi - \xi\|_{L^2(\partial D)} \|\vec{q}\|_{L^2(\partial D)} \\ &\lesssim h_D^{-\frac{1}{2}} \|Q_{k,D}^b \xi - \xi\|_{L^2(\partial D)} \|\vec{q}\|_{L^2(D)} \end{aligned} \quad (12)$$

then let $p \in \mathbb{P}_k(D)$,

$$\|Q_{k,D}^b \xi - \xi\|_{L^2(\partial D)} \lesssim \|\xi - p\|_{L^2(\partial D)}$$

so that with Lemma 2.2 and inequality (7), let p be $Q_{k,D}^0 \xi$, we have

$$h_D^{-\frac{1}{2}} \|Q_{k,D}^b \xi - \xi\|_{L^2(\partial D)} \lesssim h^k \|\xi\|_{H^{k+1}(D)}, \quad (13)$$

with (12) and (13), we get (10).

To get (11), from (9), we have

$$(\nabla_w Q_h \xi - \mathbb{Q}_{k-1,D} \nabla \xi, \vec{q})_D = \langle Q_{k,D}^b \xi - \xi, \vec{q} \cdot \vec{n} \rangle_{\partial D}$$

let $\vec{q} = \nabla_w Q_h \xi - \mathbb{Q}_{k-1,D} \nabla \xi$, with (12)

$$\begin{aligned} \|\nabla_w Q_h \xi - \mathbb{Q}_{k-1,D} \nabla \xi\|_{L^2(D)}^2 &\lesssim \langle Q_{k,D}^b \xi - \xi, \vec{q} \cdot \vec{n} \rangle_{\partial D} \\ &\lesssim h_D^{-\frac{1}{2}} \|Q_{k,D}^b \xi - \xi\|_{L^2(\partial D)} \|\nabla_w Q_h \xi - \mathbb{Q}_{k-1,D} \nabla \xi\|_{L^2(D)} \end{aligned}$$

with (13), we get (11). □

Remark 2. If edge/face $e \subset \partial D$ is part of a line/plane, then $\langle Q_{k,D}^b \xi - \xi, \vec{q} \cdot \vec{n} \rangle_e = 0$.

2.2. The Weak Galerkin Finite Element Scheme

Let Ω be a bounded domain (2D or 3D) with $C^{0,1}$ boundary or interface. Suppose \mathcal{T}_h is the partition of Ω , each element D of \mathcal{T}_h is shape-regular, and \mathcal{E}_h is the set of sides/faces in \mathcal{T}_h , $h = \max_{D \in \mathcal{T}_h} h_D$.

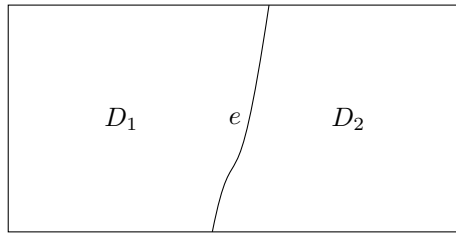


Figure 2: e is shared by two elements

Let D_0 be the inner part of D , $\mathbb{P}_k(D_0)$ be the space of polynomials on D_0 with degrees no more than k , and on each side/face, $e \in \mathcal{E}_h$, let $\mathbb{P}_k|_e$ be the space of traces of polynomials $\mathbb{P}_k(\mathbb{R}^n)$ on e , so the basis functions on shared e , see Figure 2, are uniquely determined by collecting the linearly independent traces of $\mathbb{P}_k(\mathbb{R}^n)$. For example, traces of $\mathbb{P}_1(\mathbb{R}^2)$ on e , in Figure 2, are $\{1, x, y\}$. Then the weak Galerkin finite element space is given by (14)

$$V_h := \{v : v|_{D_0} \in \mathbb{P}_k(D_0) \forall D \in \mathcal{T}_h \text{ and } v|_e \in \mathbb{P}_k|_e \forall e \in \mathcal{E}_h\}. \quad (14)$$

Let the space V_h^0 be the subspace of V_h which has vanishing boundary value on $\partial\Omega$

$$V_h^0 := \{v : v \in V_h \text{ and } v|_{\partial\Omega} = 0\}. \quad (15)$$

We then define $V_h|_D$ as the space $\{v = (v_0, v_b) : v_0 \in \mathbb{P}_k(D_0) \text{ and } v_b \in \mathbb{P}_k|_e \ \forall e \in \partial D\}$.

Lemma 2.7. *If D is shape-regular, for any $\xi \in H^{k+1}(D)$ and $v \in V_h|_D$, we have*

$$|h_D^{-1} \langle Q_{k,D}^0 \xi - Q_{k,D}^b \xi, v_0 - v_b \rangle_{\partial D}| \lesssim h_D^k \|\xi\|_{H^{k+1}(D)} h_D^{-\frac{1}{2}} \|v_0 - v_b\|_{L^2(\partial D)}, \quad (16)$$

$$|\langle (\nabla \xi - Q_{k-1,D} \nabla \xi) \cdot \vec{n}, v_0 - v_b \rangle_{\partial D}| \lesssim h_D^k \|\xi\|_{H^{k+1}(D)} h_D^{-\frac{1}{2}} \|v_0 - v_b\|_{L^2(\partial D)}, \quad (17)$$

where $k \geq 1$ and the hidden constant only depends on ρ_D and k .

Proof. To get (16), we have

$$|h_D^{-1} \langle Q_{k,D}^0 \xi - Q_{k,D}^b \xi, v_0 - v_b \rangle_{\partial D}| \lesssim h_D^{-\frac{1}{2}} \|Q_{k,D}^0 \xi - Q_{k,D}^b \xi\|_{L^2(\partial D)} h_D^{-\frac{1}{2}} \|v_0 - v_b\|_{L^2(\partial D)},$$

for the first term on the right side, we have

$$h_D^{-\frac{1}{2}} \|Q_{k,D}^0 \xi - Q_{k,D}^b \xi\|_{L^2(\partial D)} \lesssim h_D^{-\frac{1}{2}} \|Q_{k,D}^0 \xi - \xi\|_{L^2(\partial D)} + h_D^{-\frac{1}{2}} \|Q_{k,D}^b \xi - \xi\|_{L^2(\partial D)},$$

with Lemma 2.2, Lemma 2.5 and (13), then (16) is obtained.

To get (17), we have

$$|\langle (\nabla \xi - Q_{k-1,D} \nabla \xi) \cdot \vec{n}, v_0 - v_b \rangle_{\partial D}| \lesssim h_D^{\frac{1}{2}} \|\nabla \xi - Q_{k-1,D} \nabla \xi\|_{L^2(\partial D)} h_D^{-\frac{1}{2}} \|v_0 - v_b\|_{L^2(\partial D)},$$

with Lemma 2.2 and Lemma 2.5, (17) is obtained. \square

Lemma 2.8. [19] *Assume that D is shape-regular. Then we have*

$$\|\nabla v_0\|_{L^2(D)}^2 \lesssim \|\nabla_w v\|_{L^2(D)}^2 + h_D^{-1} \|v_b - v_0\|_{L^2(\partial D)}^2, \ \forall v \in V_h|_D, \quad (18)$$

the hidden constant only depends on ρ_D and k .

3. The weak Galerkin finite element method for elliptic equation

Let Ω be a bounded domain with $C^{0,1}$ boundary in \mathbb{R}^n , $f \in L^2(\Omega)$, the Poisson's equation is

$$\begin{cases} -\Delta u = f, \\ u|_{\partial\Omega} = 0. \end{cases} \quad (19)$$

For any $v \in V_h$, the weak gradient of v is defined on each element D by (3), respectively. For any $u, v \in V_h$, the bilinear form is defined as

$$a_h(u, v) = \sum_{D \in \mathcal{T}_h} \int_D \nabla_w u \cdot \nabla_w v \, dx. \quad (20)$$

The stabilization term is:

$$s_h(u, v) = \sum_{D \in \mathcal{T}_h} h_D^{-1} \langle u_0 - u_b, v_0 - v_b \rangle_{\partial D}. \quad (21)$$

A numerical solution for (19) can be obtained by seeking $u_h = (u_0, u_b) \in V_h^0$ such that

$$a_s(u_h, v) := a_h(u_h, v) + s_h(u_h, v) = (f, v_0)_\Omega, \ \forall v = (v_0, v_b) \in V_h^0. \quad (22)$$

Then the weak-1 norm of $v \in V$ is defined as

$$|v|_{k-1,w}^2 = \sum_{D \in \mathcal{T}_h} \|\nabla_w v\|_{L^2(D)}^2 + h_D^{-1} \|v_0 - v_b\|_{L^2(\partial D)}^2, \quad (23)$$

where $k \geq 1$ is an integer.

We generate Figure 3 by PolyMesher [28] to show how the mesh in 2D could be.

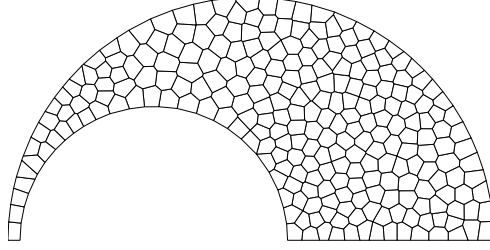


Figure 3: A shape regular partition of domain Ω

Lemma 3.1. *Suppose the partition \mathcal{T}_h is shape-regular. Then we have*

$$\|v_0\|_{L^2(\Omega)} \lesssim |v|_{k-1,w}, \quad \forall v = (v_0, v_b) \in V_h^0,$$

the hidden constant only depends on ρ_D and k .

Proof. The key to proving Lemma 3.1 is that on each edge or face e , $v|_e$ is unique. Then, same as Lemma 7.1 in [10], we have the discrete Poincaré inequality. \square

Also, we have the existence and uniqueness of the solution of (22).

3.1. Error Analysis

Let $u \in H^2(\Omega)$ be the solution of (19) and $v \in V_h^0$. Then, multiply (19) by v_0 of $v = (v_0, v_b) \in V_h^0$ we have

$$\sum_{D \in \mathcal{T}_h} (\nabla u, \nabla v_0)_D = (f, v_0)_\Omega + \sum_{D \in \mathcal{T}_h} \langle v_0 - v_b, \nabla u \cdot \vec{n} \rangle_{\partial D}, \quad (24)$$

where $\sum_{D \in \mathcal{T}_h} \langle v_b, \nabla u \cdot \vec{n} \rangle_{\partial D} = 0$.

It follows from (3), (9) and the integration by parts

$$\begin{aligned} & (\nabla_w Q_h u, \nabla_w v)_D \\ &= (\mathbb{Q}_{k-1,D} \nabla u, \nabla_w v)_D + \langle Q_{k,D}^b u - u, \nabla_w v \cdot \vec{n} \rangle_{\partial D} \\ &= -(v_0, \nabla \cdot (\mathbb{Q}_{k-1,D} \nabla u))_D + \langle v_b, (\mathbb{Q}_{k-1,D} \nabla u) \cdot \vec{n} \rangle_{\partial D} + \langle Q_{k,D}^b u - u, \nabla_w v \cdot \vec{n} \rangle_{\partial D} \\ &= (\nabla v_0, \mathbb{Q}_{k-1,D} \nabla u)_D - \langle v_0 - v_b, (\mathbb{Q}_{k-1,D} \nabla u) \cdot \vec{n} \rangle_{\partial D} + \langle Q_{k,D}^b u - u, \nabla_w v \cdot \vec{n} \rangle_{\partial D} \\ &= (\nabla u, \nabla v_0)_D - \langle v_0 - v_b, (\mathbb{Q}_{k-1,D} \nabla u) \cdot \vec{n} \rangle_{\partial D} + \langle Q_{k,D}^b u - u, \nabla_w v \cdot \vec{n} \rangle_{\partial D}. \end{aligned} \quad (25)$$

Combining (24) and (25), we have

$$\begin{aligned} \sum_{D \in \mathcal{T}_h} (\nabla_w Q_h u, \nabla_w v)_D &= (f, v_0)_\Omega + \sum_{D \in \mathcal{T}_h} \langle v_0 - v_b, (\nabla u - \mathbb{Q}_{k-1,D} \nabla u) \cdot \vec{n} \rangle_{\partial D} \\ &\quad + \sum_{D \in \mathcal{T}_h} \langle Q_{k,D}^b u - u, \nabla_w v \cdot \vec{n} \rangle_{\partial D}. \end{aligned} \quad (26)$$

Adding $s_h(Q_h u, v)$ to both sides of (26) gives

$$\begin{aligned} a_s(Q_h u, v) &= (f, v_0)_\Omega + \sum_{D \in \mathcal{T}_h} \langle v_0 - v_b, (\nabla u - \mathbb{Q}_{k-1,D} \nabla u) \cdot \vec{n} \rangle_{\partial D} \\ &\quad + \sum_{D \in \mathcal{T}_h} \langle Q_{k,D}^b u - u, \nabla_w v \cdot \vec{n} \rangle_{\partial D} + s_h(Q_h u, v). \end{aligned} \quad (27)$$

Subtracting (22) from (27), we have the error equation

$$\begin{aligned} a_s(e_h, v) &= \sum_{D \in \mathcal{T}_h} \langle v_0 - v_b, (\nabla u - \mathbb{Q}_{k-1, D} \nabla u) \cdot \vec{n} \rangle_{\partial D} \\ &\quad + \sum_{D \in \mathcal{T}_h} \langle Q_{k, D}^b u - u, \nabla_w v \cdot \vec{n} \rangle_{\partial D} + s_h(Q_h u, v). \end{aligned} \quad (28)$$

where

$$e_h|_D = (e_0, e_b)_D := (Q_{k, D}^0 u - u_0, Q_{k, D}^b u - u_b)_D = (Q_h u - u_h)|_D$$

which is the error between the weak Galerkin finite element solution (u_0, u_b) and the L^2 projection of the exact solution. Then we define a norm $\|\cdot\|_h$ as

$$\|\vec{v}\|_h^2 := \sum_{D \in \mathcal{T}_h} \|\vec{v}\|_{L^2(D)}, \quad \forall \vec{v} \in [L^2(\Omega)]^n.$$

Theorem 3.1. *Let $u_h \in V_h^0$ be the weak Galerkin finite element solution of the problem (19). Assume that the exact solution is so regular that $u \in H^{k+1}(\Omega)$. Then we have*

$$\|\nabla u - \nabla_w u_h\|_h \lesssim h^k \|u\|_{H^{k+1}(\Omega)}, \quad (29)$$

$$\|\nabla u - \nabla u_0\|_h \lesssim h^k \|u\|_{H^{k+1}(\Omega)}, \quad (30)$$

the hidden constants only depend on ρ_D and k .

Proof. Let $v = e_h$ in (28), we have

$$\begin{aligned} |e_h|_{k-1, w}^2 &= \sum_{D \in \mathcal{T}_h} \langle e_0 - e_b, (\nabla u - \mathbb{Q}_{k-1, D} \nabla u) \cdot \vec{n} \rangle_{\partial D} \\ &\quad + \sum_{D \in \mathcal{T}_h} \langle Q_{k, D}^b u - u, \nabla_w e_h \cdot \vec{n} \rangle_{\partial D} + s_h(Q_h u, e_h). \end{aligned}$$

It then follows from (10) and Lemma 2.7

$$|e_h|_{k-1, w}^2 \lesssim h^k \|u\|_{H^{k+1}(\Omega)} |e_h|_{k-1, w}. \quad (31)$$

Based on (31), firstly, we prove (29),

$$\|\nabla u - \nabla_w u_h\|_h \leq \|\nabla u - \mathbb{Q}_{k-1}(\nabla u)\|_h + \|\mathbb{Q}_{k-1}(\nabla u) - \nabla_w Q_h u\|_h + \|\nabla_w Q_h u - \nabla_w u_h\|_h,$$

with Lemma 2.5 and Lemma 2.6 and

$$\|\nabla_w(Q_h u - u_h)\|_h \leq |e_h|_{k-1, w}$$

we have (29).

Secondly, with Lemma 2.8, we have

$$\begin{aligned} \sum_{D \in \mathcal{T}_h} \|\nabla(Q_{k, D}^0 u - u_h|_{D_0})\|_{L^2(D)}^2 &= \sum_{D \in \mathcal{T}_h} \|\nabla e_0\|_{L^2(D)}^2 \\ &\leq \sum_{D \in \mathcal{T}_h} \|\nabla_w e_h\|_{L^2(D)}^2 + h_D^{-1} \|e_b - e_0\|_{L^2(\partial D)}^2 \\ &\leq |u_h - Q_h u|_{k-1, w}^2 \end{aligned}$$

which means

$$\sum_{D \in \mathcal{T}_h} \|\nabla(Q_{k, D}^0 u - u_h|_{D_0})\|_{L^2(D)}^2 \lesssim h^{2k} \|u\|_{H^{k+1}(\Omega)}^2.$$

Also by Lemma 2.5

$$\sum_{D \in \mathcal{T}_h} \|\nabla(Q_{k, D}^0 u - u)\|_{L^2(D)}^2 \lesssim h^{2k} \|u\|_{H^{k+1}(\Omega)}^2,$$

then we have (30)

$$\|\nabla u - \nabla u_0\|_h \lesssim h^k \|u\|_{H^{k+1}(\Omega)}.$$

□

Theorem 3.2. Let $u_h \in V_h^0$ be the weak Galerkin finite element solution of the problem (19). Assume that the exact solution is so regular that $u \in H^{k+1}(\Omega)$. Then we have

$$\|u - u_0\|_{L^2(\Omega)} \lesssim h^{k+1} \|u\|_{H^{k+1}(\Omega)}, \quad (32)$$

the hidden constant only depends on ρ_D and k .

Proof. We begin with a dual problem seeking $\phi \in H_0^2(\Omega)$ such that $-\Delta\phi = e_0$. Suppose we have $\|\phi\|_{H^2(\Omega)} \lesssim \|e_0\|_{L^2(\Omega)}$.

Then we have

$$\|e_0\|_{L^2(\Omega)}^2 = \sum_{D \in \mathcal{T}_h} (\nabla\phi, \nabla e_0)_D - \sum_{D \in \mathcal{T}_h} \langle \nabla\phi \cdot \vec{n}, e_0 - e_b \rangle_{\partial D}. \quad (33)$$

Let $u = \phi$ and $v = e_h$ in (25), we have

$$(\nabla\phi, \nabla e_0)_D = (\nabla_w Q_h \phi, \nabla_w e_h)_D + \langle e_0 - e_b, (\mathbb{Q}_{k-1,D} \nabla\phi) \cdot \vec{n} \rangle_{\partial D} - \langle Q_{k,D}^b \phi - \phi, \nabla_w e_h \cdot \vec{n} \rangle_{\partial D}. \quad (34)$$

Combining (33) and (34), we have

$$\begin{aligned} \|e_0\|_{L^2(\Omega)}^2 &= (\nabla_w Q_h \phi, \nabla_w e_h)_\Omega + \sum_{D \in \mathcal{T}_h} \langle (\mathbb{Q}_{k-1,D} \nabla\phi - \nabla\phi) \cdot \vec{n}, e_0 - e_b \rangle_{\partial D} \\ &\quad - \sum_{D \in \mathcal{T}_h} \langle Q_{k,D}^b \phi - \phi, \nabla_w e_h \cdot \vec{n} \rangle_{\partial D}. \end{aligned} \quad (35)$$

So that by Lemma 2.6 and Lemma 2.7, we have

$$\left| \sum_{D \in \mathcal{T}_h} \langle (\mathbb{Q}_{k-1,D} \nabla\phi - \nabla\phi) \cdot \vec{n}, e_0 - e_b \rangle_{\partial D} \right| \lesssim h \|\phi\|_{H^2(\Omega)} |e_h|_{k-1,w}, \quad (36)$$

$$\left| \sum_{D \in \mathcal{T}_h} \langle Q_{k,D}^b \phi - \phi, \nabla_w e_h \cdot \vec{n} \rangle_{\partial D} \right| \lesssim h \|\phi\|_{H^2(\Omega)} |e_h|_{k-1,w}. \quad (37)$$

Then let $v = Q_h \phi$ in (28), such that

$$\begin{aligned} (\nabla_w Q_h \phi, \nabla_w e_h)_\Omega &= \sum_{D \in \mathcal{T}_h} \langle Q_{k,D}^0 \phi - Q_{k,D}^b \phi, (\nabla u - \mathbb{Q}_{k-1,D} \nabla u) \cdot \vec{n} \rangle_{\partial D} \\ &\quad + \sum_{D \in \mathcal{T}_h} \langle Q_{k,D}^b u - u, (\nabla_w Q_h \phi - \nabla\phi) \cdot \vec{n} \rangle_{\partial D} \\ &\quad + s_h(Q_h u, Q_h \phi) - s_h(e_h, Q_h \phi), \end{aligned}$$

where

$$\sum_{D \in \mathcal{T}_h} \langle Q_{k,D}^b u - u, \nabla\phi \cdot \vec{n} \rangle_{\partial D} = 0.$$

Same as the proof of Theorem 8.2 in [10], we have

$$\sum_{D \in \mathcal{T}_h} \langle Q_{k,D}^0 \phi - Q_{k,D}^b \phi, (\nabla u - \mathbb{Q}_{k-1,D} \nabla u) \cdot \vec{n} \rangle_{\partial D} \lesssim h^{k+1} \|u\|_{H^{k+1}(\Omega)} \|\phi\|_{H^2(\Omega)}$$

and

$$|s_h(Q_h u, Q_h \phi)| + |s_h(e_h, Q_h \phi)| \lesssim h^{k+1} \|u\|_{H^{k+1}(\Omega)} \|\phi\|_{H^2(\Omega)}.$$

Then

$$|\langle Q_{k,D}^b u - u, (\nabla_w Q_h \phi - \nabla\phi) \cdot \vec{n} \rangle_{\partial D}| \lesssim h_D^{-\frac{1}{2}} \|Q_{k,D}^b u - u\|_{L^2(\partial D)} h_D^{\frac{1}{2}} \|\nabla_w Q_h \phi - \nabla\phi\|_{L^2(\partial D)},$$

where

$$\begin{aligned}
& h_D^{\frac{1}{2}} \|\nabla_w Q_h \phi - \nabla \phi\|_{L^2(\partial D)} \\
& \lesssim h_D^{\frac{1}{2}} \|\nabla_w Q_h \phi - \mathbb{Q}_{k-1,D} \nabla \phi\|_{L^2(\partial D)} + h_D^{\frac{1}{2}} \|\mathbb{Q}_{k-1,D} \nabla \phi - \nabla \phi\|_{L^2(\partial D)} \\
& \lesssim \|\nabla_w Q_h \phi - \mathbb{Q}_{k-1,D} \nabla \phi\|_{L^2(D)} + h_D \|\nabla_w Q_h \phi - \mathbb{Q}_{k-1,D} \nabla \phi\|_{H^1(D)} \\
& \quad + h_D^{\frac{1}{2}} \|\mathbb{Q}_{k-1,D} \nabla \phi - \nabla \phi\|_{L^2(\partial D)} \\
& \lesssim h_D \|\phi\|_{H^2(D)} + \|\nabla_w Q_h \phi - \mathbb{Q}_{k-1,D} \nabla \phi\|_{L^2(D)} \\
& \quad + h_D^{\frac{1}{2}} \|\mathbb{Q}_{k-1,D} \nabla \phi - \nabla \phi\|_{L^2(\partial D)} \\
& \lesssim h_D \|\phi\|_{H^2(D)}
\end{aligned}$$

by Lemma 2.2, Lemma 2.3, Lemma 2.5 and Lemma 2.6

$$|\langle Q_{k,D}^b u - u, (\nabla_w Q_h \phi - \nabla \phi) \cdot \vec{n} \rangle_{\partial D}| \lesssim h_D^{k+1} \|u\|_{H^{k+1}(D)} \|\phi\|_{H^2(D)}.$$

Then

$$|(\nabla_w Q_h \phi, \nabla_w e_h)_\Omega| \lesssim h^{k+1} \|u\|_{H^{k+1}(\Omega)} \|\phi\|_{H^2(\Omega)}. \quad (38)$$

By (31), (35), (36), (37) and (38), we have

$$\|Q_k^0 u - u_0\|_{L^2(\Omega)} \lesssim h^{k+1} \|u\|_{H^{k+1}(\Omega)},$$

with

$$\|Q_k^0 u - u\|_{L^2(\Omega)} \lesssim h^{k+1} \|u\|_{H^{k+1}(\Omega)},$$

the error estimate (32) is obtained. \square

4. The weak Galerkin finite element method for elliptic interface problem

Let Ω be a bounded domain with $C^{0,1}$ boundary in \mathbb{R}^n , $n = 2, 3$, $\Gamma \subset \Omega$ be the $C^{0,1}$ interface (Fig.4), $f \in L^2(\Omega)$, the equation is

$$\begin{cases}
-\nabla \cdot (\beta \nabla u) & = f, \\
[u]_\Gamma & = 0, \\
(\beta_1 \nabla u \cdot \vec{n} - \beta_2 \nabla u \cdot \vec{n})|_\Gamma & = g, \\
u|_{\partial\Omega} & = 0,
\end{cases} \quad (39)$$

where \vec{n} is the outward normal vector to $\partial\Omega_1$, β_1, β_2 are two positive constants defined on Ω_1 and Ω_2 respectively. For simplicity, let $[u]_\Gamma := u_1|_\Gamma - u_2|_\Gamma = 0$.

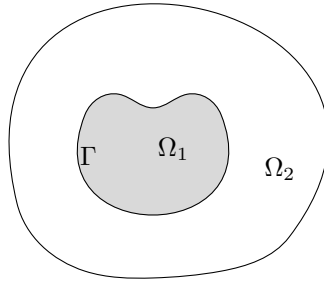


Figure 4: A domain $\Omega = \Omega_1 \cup \Gamma \cup \Omega_2$ with $C^{0,1}$ interface Γ

The mesh \mathcal{T}_h contains shape-regular curvilinear polygons or polyhedrons which have edges or faces as parts of $\partial\Omega$ or Γ , and there is no element cross Γ . Here we use the same weak Galerkin finite element schemes

as in Section 2.2. For any $v \in V_h$, the weak gradient of v is defined on each element D by (3), respectively. For any $u, v \in V_h$, the bilinear form is defined by $b_h(u, v)$

$$b_h(u, v) = \sum_{D \in \mathcal{T}_h} \int_D \beta \nabla_w u \cdot \nabla_w v \, dx. \quad (40)$$

The stabilization term is:

$$s_h(u, v) = \sum_{D \in \mathcal{T}_h} h_D^{-1} \langle u_0 - u_b, v_0 - v_b \rangle_{\partial D}. \quad (41)$$

A numerical solution for (39) can be obtained by seeking $u_h = (u_0, u_b) \in V_h^0$ such that

$$b_s(u_h, v) = (f, v_0)_\Omega + \langle g, v_b \rangle_\Gamma, \quad \forall v = (v_0, v_b) \in V_h^0. \quad (42)$$

where $b_s(u_h, v) := b_h(u_h, v) + s_h(u_h, v)$. Then we define a new weak norm as

$$\|v\| = (b_s(v, v))^{\frac{1}{2}}, \quad \forall v \in V_h^0. \quad (43)$$

Also, we have the existence and uniqueness of the solution of (39) as in [11].

4.1. Error Analysis

Let $u \in H_0^1(\Omega)$ and $u|_{\Omega_i} \in H^2(\Omega_i)$, $i = 1, 2$, be the solution of (39) and $v \in V_h^0$. Then, multiply (39) by v_0 of $v = (v_0, v_b) \in V_h^0$ we have

$$\sum_{D \in \mathcal{T}_h} (\beta \nabla u, \nabla v_0)_D = (f, v_0)_\Omega + \langle g, v_b \rangle_\Gamma + \sum_{D \in \mathcal{T}_h} \langle v_0 - v_b, \beta \nabla u \cdot \vec{n} \rangle_{\partial D}, \quad (44)$$

where $\sum_{D \in \mathcal{T}_h} \langle v_b, \beta \nabla u \cdot \vec{n} \rangle_{\partial D} = \sum_{e \in \Gamma} \langle g, v_b \rangle_e$.

It follows from (3), (9) and the integration by parts

$$\begin{aligned} (\beta \nabla_w Q_h u, \nabla_w v)_D &= (\beta Q_{k-1, D} \nabla u, \nabla_w v)_D + \langle Q_{k, D}^b u - u, \beta \nabla_w v \cdot \vec{n} \rangle_{\partial D} \\ &= (\beta \nabla u, \nabla v_0)_D - \langle v_0 - v_b, \beta (Q_{k-1, D} \nabla u) \cdot \vec{n} \rangle_{\partial D} \\ &\quad + \langle Q_{k, D}^b u - u, \beta \nabla_w v \cdot \vec{n} \rangle_{\partial D}. \end{aligned} \quad (45)$$

Combining (44) and (45), adding $s_h(Q_h u, v)$ to both sides, we have

$$\begin{aligned} b_s(Q_h u, v) &= (f, v_0)_\Omega + \langle g, v_b \rangle_\Gamma + \sum_{D \in \mathcal{T}_h} \langle v_0 - v_b, \beta (\nabla u - Q_{k-1, D} \nabla u) \cdot \vec{n} \rangle_{\partial D} \\ &\quad + \sum_{D \in \mathcal{T}_h} \langle Q_{k, D}^b u - u, \beta \nabla_w v \cdot \vec{n} \rangle_{\partial D} + s_h(Q_h u, v). \end{aligned} \quad (46)$$

Subtracting (42) from (46), we have the error equation

$$\begin{aligned} b_s(e_h, v) &= \sum_{D \in \mathcal{T}_h} \langle v_0 - v_b, \beta (\nabla u - Q_{k-1, D} \nabla u) \cdot \vec{n} \rangle_{\partial D} \\ &\quad + \sum_{D \in \mathcal{T}_h} \langle Q_{k, D}^b u - u, \beta \nabla_w v \cdot \vec{n} \rangle_{\partial D} + s_h(Q_h u, v). \end{aligned} \quad (47)$$

where

$$e_h|_D = (e_0, e_b)_D := (Q_{k, D}^0 u - u_0, Q_{k, D}^b u - u_b)_D = (Q_h u - u_h)|_D$$

which is the error between the weak Galerkin finite element solution (u_0, u_b) and the L^2 projection of the exact solution. Then we define a norm $\|\cdot\|_\beta$ as

$$\|\vec{v}\|_\beta^2 := \sum_{D \in \mathcal{T}_h} (\beta \vec{v}, \vec{v})_D, \quad \forall \vec{v} \in [L^2(\Omega)]^n,$$

and suppose $v \in H^1(\Omega)$, $v|_{\Omega_i} \in H^{k+1}(\Omega_i)$, $i = 1, 2$, we define

$$\|v\|_{k+1, \Omega}^2 = \|v\|_{H^{k+1}(\Omega_1)}^2 + \|v\|_{H^{k+1}(\Omega_2)}^2.$$

Theorem 4.1. Let $u_h \in V_h^0$ be the weak Galerkin finite element solution of the problem (39). Assume that the exact solution is so regular that $u|_{\Omega_i} \in H^{k+1}(\Omega_i), i = 1, 2$. Then we have

$$\|\nabla u - \nabla_w u_h\|_\beta \lesssim h^k \|u\|_{k+1, \Omega}, \quad (48)$$

$$\|\nabla u - \nabla u_0\|_\beta \lesssim h^k \|u\|_{k+1, \Omega}, \quad (49)$$

the hidden constants only depend on ρ_D and k .

Proof. Let $v = e_h$ in (47), we have

$$|||e_h||| = \sum_{D \in \mathcal{T}_h} \langle e_0 - e_b, \beta(\nabla u - \mathbb{Q}_{k-1, D} \nabla u) \cdot \vec{n} \rangle_{\partial D} + \sum_{D \in \mathcal{T}_h} \langle Q_{k, D}^b u - u, \beta \nabla_w e_h \cdot \vec{n} \rangle_{\partial D} + s_h(Q_h u, e_h). \quad (50)$$

It then follows from (10) and Lemma 2.7

$$|||e_h|||^2 \lesssim h^k \|u\|_{k+1, \Omega} |||e_h|||. \quad (51)$$

Based on (51), firstly, we prove (48),

$$\|\nabla u - \nabla_w u_h\|_\beta \leq \|\nabla u - \mathbb{Q}_{k-1} \nabla u\|_\beta + \|\mathbb{Q}_{k-1} \nabla u - \nabla_w Q_h u\|_\beta + \|\nabla_w Q_h u - \nabla_w u_h\|_\beta,$$

with Lemma 2.5 and Lemma 2.6 and

$$\|\nabla_w(Q_h u - u_h)\|_\beta \leq |||e_h|||$$

we have (29).

Secondly, with Lemma 2.8, we have

$$\begin{aligned} \sum_{D \in \mathcal{T}_h} \|\beta \nabla(Q_{k, D}^0 u - u_h|_{D_0})\|_{L^2(D)}^2 &= \sum_{D \in \mathcal{T}_h} \|\beta \nabla e_0\|_{L^2(D)}^2 \\ &\lesssim \sum_{D \in \mathcal{T}_h} \|\beta \nabla_w e_h\|_{L^2(D)}^2 + h_D^{-1} \|e_b - e_0\|_{L^2(\partial D)}^2 \\ &\lesssim |||e_h|||^2 \end{aligned}$$

which means

$$\sum_{D \in \mathcal{T}_h} \|\beta \nabla(Q_{k, D}^0 u - u_h|_{D_0})\|_{L^2(D)}^2 \lesssim h^{2k} \|u\|_{k+1, \Omega}^2.$$

Also with Lemma 2.5

$$\sum_{D \in \mathcal{T}_h} \|\beta \nabla(Q_{k, D}^0 u - u)\|_{L^2(D)}^2 \lesssim h^{2k} \|u\|_{k+1, \Omega}^2,$$

so that we have (49)

$$\|\nabla u - \nabla u_0\|_\beta \lesssim h^k \|u\|_{k+1, \Omega}.$$

□

Theorem 4.2. Let $u_h \in V_h$ be the weak Galerkin finite element solution of the problem (39). Assume that the exact solution is so regular that $u|_{\Omega_i} \in H^{k+1}(\Omega_i), i = 1, 2$. Then we have

$$\|u - u_0\|_{L^2(\Omega)} \lesssim h^{k+1} \|u\|_{k+1, \Omega}, \quad (52)$$

the hidden constant only depends on ρ_D and k .

Proof. We begin with a dual problem seeking $\phi \in H_0^1(\Omega)$ such that $-\nabla \cdot (\beta \nabla \phi) = e_0$, and $g = 0$ as in (39). Suppose we have $\|\phi\|_{2, \Omega} \lesssim \|e_0\|_{L^2(\Omega)}$.

Then we have

$$\|e_0\|_{L^2(\Omega)}^2 = \sum_{D \in \mathcal{T}_h} (\beta \nabla \phi, \nabla e_0)_D - \sum_{D \in \mathcal{T}_h} \langle \beta \nabla \phi \cdot \vec{n}, e_0 - e_b \rangle_{\partial D}. \quad (53)$$

Let $u = \phi$ and $v = e_h$ in (45), we have

$$\begin{aligned} (\beta \nabla \phi, \nabla e_0)_D &= (\beta \nabla_w Q_h \phi, \nabla_w e_h)_D + \langle e_0 - e_b, \beta(\mathbb{Q}_{k-1,D} \nabla \phi) \cdot \vec{n} \rangle_{\partial D} \\ &\quad - \langle Q_{k,D}^b \phi - \phi, \beta \nabla_w e_h \cdot \vec{n} \rangle_{\partial D}. \end{aligned} \quad (54)$$

Combining (53) and (54), we have

$$\begin{aligned} \|e_0\|_{L^2(\Omega)}^2 &= (\beta \nabla_w Q_h \phi, \nabla_w e_h)_\Omega + \sum_{D \in \mathcal{T}_h} \langle \beta(\mathbb{Q}_{k-1,D} \nabla \phi - \nabla \phi) \cdot \vec{n}, e_0 - e_b \rangle_{\partial D} \\ &\quad - \sum_{D \in \mathcal{T}_h} \langle Q_{k,D}^b \phi - \phi, \beta \nabla_w e_h \cdot \vec{n} \rangle_{\partial D}. \end{aligned} \quad (55)$$

By Lemma 2.6 and Lemma 2.7, we have

$$\left| \sum_{D \in \mathcal{T}_h} \langle \beta(\mathbb{Q}_{k-1,D} \nabla \phi - \nabla \phi) \cdot \vec{n}, e_0 - e_b \rangle_{\partial D} \right| \lesssim h \|\phi\|_{2,\Omega} \|e_h\|, \quad (56)$$

$$\left| \sum_{D \in \mathcal{T}_h} \langle Q_{k,D}^b \phi - \phi, \beta \nabla_w e_h \cdot \vec{n} \rangle_{\partial D} \right| \lesssim h \|\phi\|_{2,\Omega} \|e_h\|. \quad (57)$$

Then let $v = Q_h \phi$ in (47)

$$\begin{aligned} (\beta \nabla_w Q_h \phi, \nabla_w e_h)_\Omega &= \sum_{D \in \mathcal{T}_h} \langle Q_{k,D}^0 \phi - Q_{k,D}^b \phi, \beta(\nabla u - \mathbb{Q}_{k-1,D} \nabla u) \cdot \vec{n} \rangle_{\partial D} \\ &\quad + \sum_{D \in \mathcal{T}_h} \langle Q_{k,D}^b u - u, \beta(\nabla_w Q_h \phi - \nabla \phi) \cdot \vec{n} \rangle_{\partial D} \\ &\quad + s_h(Q_h u, Q_h \phi) - s_h(e_h, Q_h \phi), \end{aligned}$$

where

$$\sum_{D \in \mathcal{T}_h} \langle Q_{k,D}^b u - u, \beta \nabla \phi \cdot \vec{n} \rangle_{\partial D} = 0.$$

Same as the proof of Theorem 8.2 in [10], we have

$$\sum_{D \in \mathcal{T}_h} \langle Q_{k,D}^0 \phi - Q_{k,D}^b \phi, \beta(\nabla u - \mathbb{Q}_{k-1,D} \nabla u) \cdot \vec{n} \rangle_{\partial D} \lesssim h^{k+1} \|u\|_{k+1,\Omega} \|\phi\|_{2,\Omega}$$

and

$$|s_h(Q_h u, Q_h \phi)| + |s_h(e_h, Q_h \phi)| \lesssim h^{k+1} \|u\|_{k+1,\Omega} \|\phi\|_{2,\Omega}.$$

Then by Lemma 2.3, Lemma 2.5, Lemma 2.6

$$|\langle Q_{k,D}^b u - u, \beta(\nabla_w Q_h \phi - \nabla \phi) \cdot \vec{n} \rangle_{\partial D}| \lesssim h_D^{-\frac{1}{2}} \|Q_{k,D}^b u - u\|_{L^2(\partial D)} \beta h_D^{\frac{1}{2}} \|\nabla_w Q_h \phi - \nabla \phi\|_{L^2(\partial D)},$$

where

$$\begin{aligned} h_D^{\frac{1}{2}} \|\nabla_w Q_h \phi - \nabla \phi\|_{L^2(\partial D)} &\lesssim h_D^{\frac{1}{2}} \|\nabla_w Q_h \phi - \mathbb{Q}_{k-1,D} \nabla \phi\|_{L^2(\partial D)} + h_D^{\frac{1}{2}} \|\mathbb{Q}_{k-1,D} \nabla \phi - \nabla \phi\|_{L^2(\partial D)} \\ &\lesssim \|\nabla_w Q_h \phi - \mathbb{Q}_{k-1,D} \nabla \phi\|_{L^2(D)} + h_D \|\nabla_w Q_h \phi - \mathbb{Q}_{k-1,D} \nabla \phi\|_{H^1(D)} \\ &\quad + h_D^{\frac{1}{2}} \|\mathbb{Q}_{k-1,D} \nabla \phi - \nabla \phi\|_{L^2(\partial D)} \\ &\lesssim h_D \|\phi\|_{H^2(D)} + \|\nabla_w Q_h \phi - \mathbb{Q}_{k-1,D} \nabla \phi\|_{L^2(D)} \\ &\quad + h_D^{\frac{1}{2}} \|\mathbb{Q}_{k-1,D} \nabla \phi - \nabla \phi\|_{L^2(\partial D)} \\ &\lesssim h_D \|\phi\|_{H^2(D)} \end{aligned}$$

so that $|\langle Q_{k,D}^b u - u, \beta(\nabla_w Q_h \phi - \nabla \phi) \cdot \vec{n} \rangle_{\partial D}| \lesssim h_D^{k+1} \|u\|_{H^{k+1}(D)} \|\phi\|_{H^2(D)}$.

Then we have

$$|(\beta \nabla_w Q_h \phi, \nabla_w e_h)_\Omega| \lesssim h^{k+1} \|u\|_{k+1,\Omega} \|\phi\|_{2,\Omega}. \quad (58)$$

By (51), (55), (56), (57) and (58), we have

$$\|Q_k^0 u - u_0\|_{L^2(\Omega)} \lesssim h^{k+1} \|u\|_{k+1, \Omega},$$

with

$$\|Q_k^0 u - u\|_{L^2(\Omega)} \lesssim h^{k+1} \|u\|_{k+1, \Omega},$$

the error estimate (52) is obtained. \square

5. Numerical Experiments

In this section, we focus on 2D problems with curved boundaries or interfaces. The main difference compared with the classical weak Galerkin method is the construction of basis functions on curved sides. For the following tests, each element in the mesh has four sides, and one or more sides are curves. We choose two types of curved sides, the special Lipschitz continuous ones formed by connecting points with short lines, and the smooth ones. Basis functions are linearly independent traces of $\mathbb{P}_k(\mathbb{R}^2)$ on the curved side, for example, it's easy to prove if the side is not straight, P_1 basis functions are always chosen: $1, x, y$. Let $x^0 = y^0 = 1$, and the set of traces for $\mathbb{P}_k(\mathbb{R}^2)$, $k \geq 2$ on the side be

$$T(\mathbb{P}_k) := \{x^i y^j | 0 \leq i, j \text{ and } i + j \leq k\}.$$

Instead of determining if the traces are linearly independent analytically, in practice, we can let (x_m, y_m) , $1 \leq m \leq M$ be sample points on the curved side, the number of those points should be sufficiently large. For each $v(x, y) \in T(\mathbb{P}_k)$, we can get a vector

$$(v(x_1, y_1), v(x_2, y_2), \dots, v(x_M, y_M)),$$

then collect all those vectors and choose the linearly independent ones, the corresponding traces are basis functions on the curved side. Numerical integration on the curved side or curvilinear element is simple, we just need to make sure it is accurate enough to calculate convergence rates. The algorithm in 2D can be easily generalized to 3D problems.

5.1. Poisson's Equation

This subsection is to verify that elements with Lipschitz continuous or smooth curved edges can also guarantee optimal convergence rates for solving Poisson's equation as long as they satisfy the shape-regular assumptions. Let

$$u(x, y) = \sin(\pi x) \sin(\pi y)$$

be the exact solution to Poisson's equation on a given domain with Dirichlet/Neumann Boundary conditions, we use P_1 and P_2 elements in Example 5.1.1 to Example 5.1.5.

Example 5.1.1. *Let the domain be $[0, 1] \times [0, 1]$, see Figure 5. We consider Poisson's equation with the Dirichlet boundary condition (on the blue lines). In the mesh, each element has a Lipschitz continuous curved side which contains three short lines, basis functions are defined on the whole green-colored curved side, there are three for P_1 element and six for P_2 element. From Table 1, we can see the convergence rates for L^2 and H^1 errors are optimal.*

Example 5.1.2. *Following Example 5.1.1, we define a parameter M which makes the curved side more flat if it is increasing, see Figure 5 (the middle one with $M = 10$) and Figure 6. For the same Poisson's equation and P_1 element, we test the condition numbers of the stiff matrices on coarse meshes and obtain the convergence rates with fixed M and refined meshes. We observe that the condition number of the stiff matrix is increasing as M increases, see Table 2. However, from Table 3, we can see that the convergence rates for L^2 and H^1 errors are still optimal (even slightly better compared with Table 1 with P_1 element). So large condition numbers do not necessarily reduce the accuracy.*

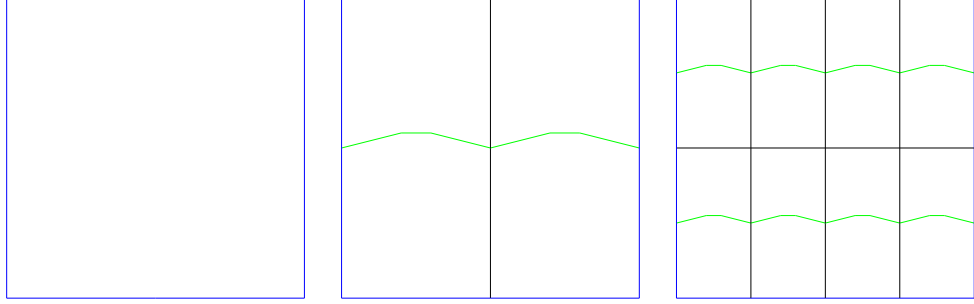


Figure 5: Example 5.1.1. Left: domain; Middle: initial mesh; Right: refined mesh

Table 1: Example 5.1.1. Convergence Rates for P_1 and P_2 Elements, $d \approx \sqrt{2}$

$h \approx$	L^2 error	P_1	H^1 error	P_1	L^2 error	P_2	H^1 error	P_2
$d/2$	4.826e-01	Rate	1.758e+00	Rate	1.516e-01	Rate	1.256e+00	Rate
$d/4$	1.396e-01	1.79	7.943e-01	1.15	1.825e-02	3.05	3.017e-01	2.06
$d/8$	3.630e-02	1.94	3.711e-01	1.10	2.112e-03	3.11	7.155e-02	2.08
$d/16$	9.167e-03	1.99	1.815e-01	1.03	2.558e-04	3.05	1.754e-02	2.03
$d/32$	2.298e-03	2.00	9.019e-02	1.01	3.169e-05	3.01	4.360e-03	2.01
$d/64$	5.748e-04	2.00	4.503e-02	1.00	3.952e-06	3.00	1.089e-03	2.00

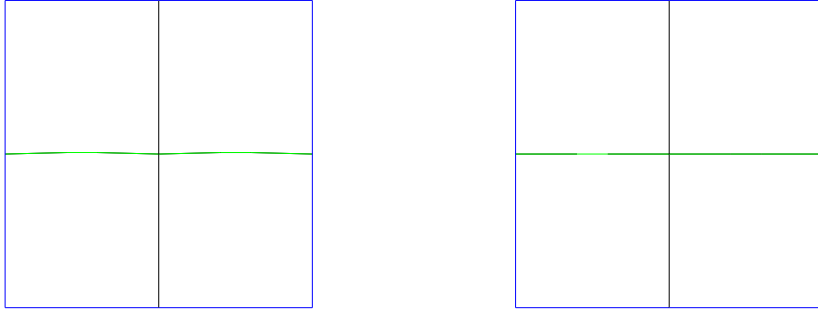


Figure 6: Example 5.1.2. Meshes with 4 elements, left: $M = 10^2$; right: $M = 10^4$

Table 2: Example 5.1.2. Condition Numbers for stiff matrices on coarse meshes with P_1 basis functions

$h \approx$	$M = 5$	$M = 10$	$M = 10^2$	$M = 10^3$	$M = 10^4$
$\sqrt{2}/2$	2.5861e+03	9.9975e+03	9.8530e+05	9.8446e+07	9.8438e+09
$\sqrt{2}/4$	1.0442e+04	3.7529e+04	3.6133e+06	3.6097e+08	3.6094e+10
$\sqrt{2}/8$	1.3266e+05	1.4676e+05	1.3561e+07	1.3547e+09	1.3547e+11

Example 5.1.3. Let the domain be $[0, 1] \times [0, 1]$, see Figure 7. Still, we consider Poisson's equation with the Dirichlet boundary condition (on the blue lines). In the mesh, each element has a smooth curved side which is part of a quadratic function, basis functions are defined on the green-colored smooth curved side, there are three for P_1 element, and five for P_2 element. From Table 4, we can see the convergence rates for L^2 and H^1 errors are optimal.

Table 3: Example 5.1.2. Errors for P_1 Element with $M = 10^2$ and $M = 10^4$, $d \approx \sqrt{2}$

$h \approx$	L^2 error	10^2	H^1 error	10^2	L^2 error	10^4	H^1 error	10^4
d/2	4.785e-01	Rate	1.760e+00	Rate	4.785e-01	Rate	1.760e+00	Rate
d/4	1.378e-01	1.80	7.868e-01	1.16	1.378e-01	1.80	7.867e-01	1.16
d/8	3.572e-02	1.95	3.674e-01	1.10	3.572e-02	1.95	3.673e-01	1.10
d/16	9.012e-03	1.99	1.796e-01	1.03	9.010e-03	1.99	1.795e-01	1.03
d/32	2.258e-03	2.00	8.923e-02	1.01	2.258e-03	2.00	8.922e-02	1.01
d/64	5.648e-04	2.00	4.455e-02	1.00	5.647e-04	2.00	4.454e-02	1.00

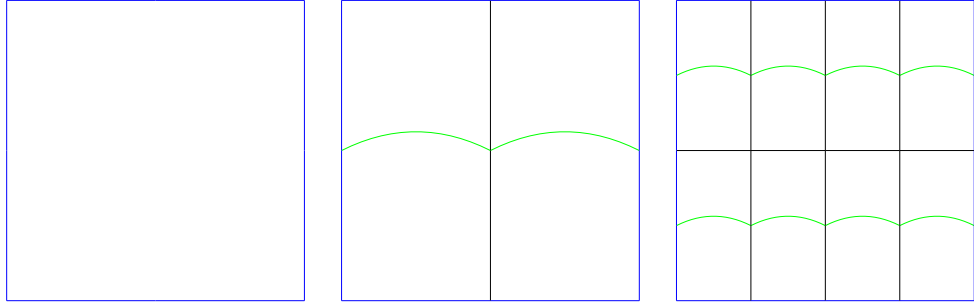


Figure 7: Example 5.1.3. Left: domain; Middle: initial mesh; Right: refined mesh

Example 5.1.4. Domain with Lipschitz continuous boundaries, let $N = 192$ and

$$x_i = r \sin(\theta_i), \quad y_i = r \cos(\theta_i); \quad \theta_i = \frac{\pi}{N}, \quad i = 0, 1, \dots, N$$

if $r = 1$, then connect points (x_i, y_i) and (x_{i+1}, y_{i+1}) by straight lines, we obtain the curve C_0 (blue color); similarly, for $r = 1.2$, we have curve C_1 (red color), the domain is bounded by C_0 and C_1 , points are marked on curves, see Figure 8. We consider Poisson's equation with the Dirichlet boundary condition on the blue curve and the Neumann Boundary condition on the red curve. In Figure 8, each element has at least one Lipschitz continuous curved side which contains multiple short lines, basis functions are defined on the whole curved side. From Table 5, we can see the convergence rates for L^2 and H^1 errors are optimal.

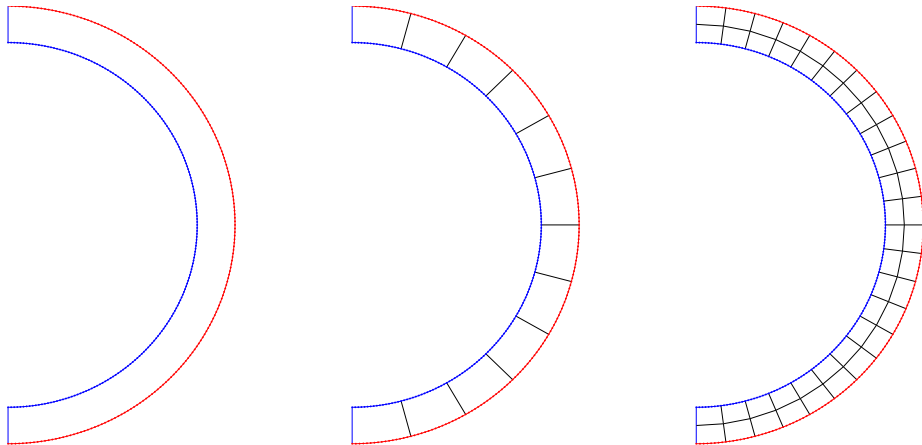


Figure 8: Example 5.1.4. Left: domain; Middle: initial mesh; Right: refined mesh

Table 4: Example 5.1.3. Convergence Rates for P_1 and P_2 Elements, $d \approx \sqrt{2}$

$h \approx$	L^2 error	P_1	H^1 error	P_1	L^2 error	P_2	H^1 error	P_2
d/2	4.871e-01	Rate	1.757	Rate	1.526e-01	Rate	1.266	Rate
d/4	1.414e-01	1.78	8.003e-01	1.13	1.864e-02	3.03	3.082e-01	2.04
d/8	3.683e-02	1.94	3.743e-01	1.10	2.183e-03	3.09	7.387e-02	2.06
d/16	9.309e-03	1.98	1.831e-01	1.03	2.661e-04	3.04	1.819e-02	2.02
d/32	2.334e-03	2.00	9.100e-02	1.01	3.303e-05	3.01	4.531e-03	2.01
d/64	5.839e-04	2.00	4.543e-02	1.00	4.121e-06	3.00	1.131e-03	2.00

Table 5: Example 5.1.4. Convergence Rates for P_1 and P_2 Elements, $d \approx 0.70$

$h \approx$	L^2 error	P_1	H^1 error	P_1	L^2 error	P_2	H^1 error	P_2
d/2	5.407e-02	Rate	7.279e-01	Rate	2.263e-02	Rate	4.034e-01	Rate
d/4	1.649e-02	1.71	3.172e-01	1.20	3.168e-03	2.84	1.044e-01	1.95
d/8	4.213e-03	1.97	1.465e-01	1.11	4.368e-04	2.86	2.740e-02	1.93
d/16	1.051e-03	2.00	7.038e-02	1.06	5.737e-05	2.93	7.049e-03	1.96
d/32	2.624e-04	2.00	3.468e-02	1.02	7.302e-06	2.97	1.783e-03	1.98

Example 5.1.5. Domain with smooth curved boundaries:

$$\Omega := \{(x, y) | x = r \sin(\theta), y = r \cos(\theta), 1 \leq r \leq 1.2, 0 \leq \theta \leq \pi\}.$$

On this domain, we consider Poisson's equation with the Dirichlet boundary condition on the blue curve and the Neumann Boundary condition on the red curve, see Figure 9. In Figure 9, each element has at least one smooth curved side, basis functions are defined on the curved side. From Table 6, we can see the convergence rates for L^2 and H^1 errors are optimal.

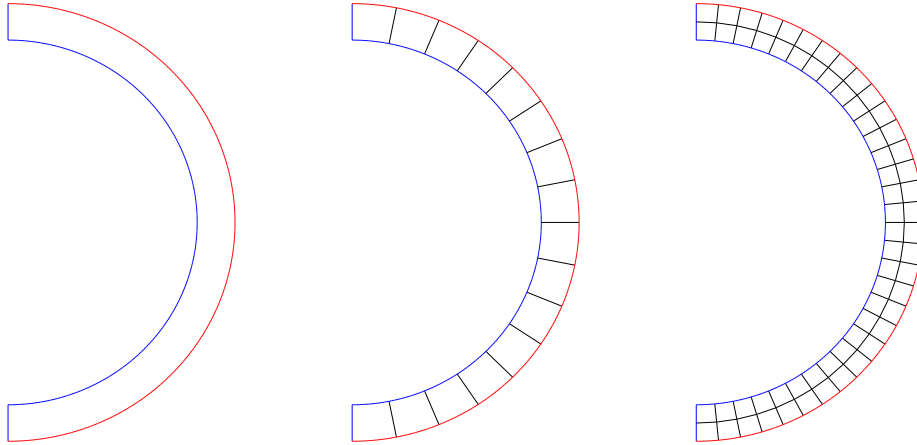


Figure 9: Example 5.1.5. Left: domain; Middle: initial mesh; Right: refined mesh

5.2. Elliptic Interface Problem

Let $\beta_1 = \beta_2 = 1$ and the exact solution be

$$u = \begin{cases} \sin(\pi x) \sin(\pi y) - 1, & \text{on } \Omega_1 \\ \sin(\pi x) \sin(\pi y), & \text{on } \Omega_2 \end{cases}$$

Table 6: Example 5.1.5. Convergence Rates for P_1 and P_2 Elements, $d \approx 0.58$

$h \approx$	L^2 error	P_1	H^1 error	P_1	L^2 error	P_2	H^1 error	P_2
d/2	3.548e-02	Rate	5.707e-01	Rate	1.582e-02	Rate	3.052e-01	Rate
d/4	1.158e-02	1.62	2.507e-01	1.19	2.086e-03	2.92	7.838e-02	1.96
d/8	3.029e-03	1.93	1.167e-01	1.10	2.722e-04	2.94	2.020e-02	1.96
d/16	7.645e-04	1.99	5.656e-02	1.04	3.474e-05	2.97	5.130e-03	1.98
d/32	1.915e-04	2.00	2.800e-02	1.01	4.377e-06	2.99	1.291e-03	1.99

for (39) with non-homogeneous jump condition. Suppose $r_0 = 1, r_1 = 1.12, r_2 = 1.24, r_3 = 1.36$, then we use P_1, P_2 elements in examples 5.2.1 and 5.2.2. Except for the new basis functions, the employed numerical scheme is the same as in [11].

Example 5.2.1. Domain with Lipschitz continuous boundaries/interfaces, let $N = 192$ and

$$x_i = r \sin(\theta_i), y_i = r \cos(\theta_i); \theta_i = \frac{\pi}{N}, i = 0, 1, \dots, N$$

if $r = r_0$, then connect points (x_i, y_i) and (x_{i+1}, y_{i+1}) by straight lines, we obtain the curve C_0 ; similarly, for $r = r_1, r_2, r_3$, we have curves C_1, C_2, C_3 . The points are marked on curves in Figure 10. Ω_1 is the region between C_1 and C_2 , the two red curves in the left domain of Figure 10; Ω_2 is the whole region with boundaries C_0 and C_3 , excluding Ω_1 . We consider the elliptic interface problem with the Dirichlet boundary condition on the blue curve. In Figure 10, each element has at least one Lipschitz continuous curved side which contains multiple short lines. Basis functions are defined on the whole curved side. From Table 7, we can see the convergence rates for L^2 and H^1 errors are optimal.

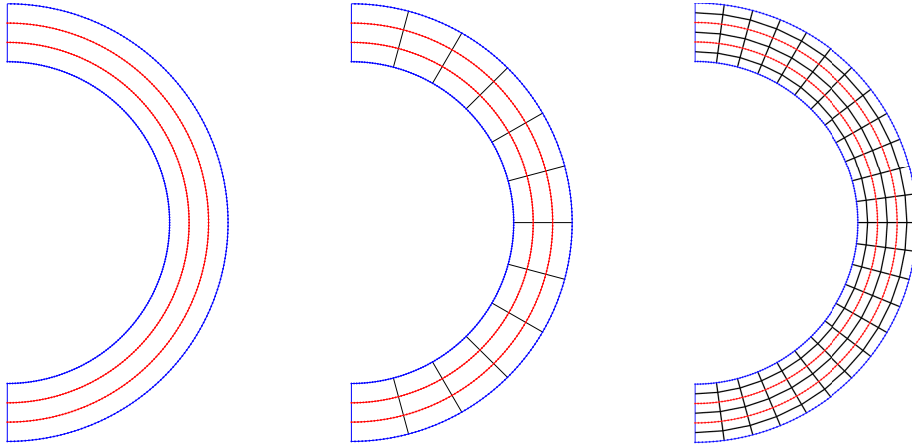


Figure 10: Example 5.2.1. Left: domain; Middle: initial mesh; Right: refined mesh

Example 5.2.2. Domain with smooth curved boundaries and interfaces:

$$\Omega_1 := \{(x, y) | x = r \sin(\theta), y = r \cos(\theta), r_1 \leq r \leq r_2, 0 \leq \theta \leq \pi\}$$

$$\Omega_2 := \{(x, y) | x = r \sin(\theta), y = r \cos(\theta), r \in [r_0, r_1] \cup [r_2, r_3], 0 \leq \theta \leq \pi\}.$$

We consider the elliptic interface problem with the Dirichlet boundary condition on the blue curve, see Figure 11. In Figure 11, each element has at least one smooth curved side. Basis functions are defined on the curved side. From Table 8, we can see the convergence rates for L^2 and H^1 errors are optimal.

Table 7: Example 5.2.1. Convergence Rates for P_1 and P_2 Elements, $d \approx 0.72$

$h \approx$	L^2 error	P_1	H^1 error	P_1	L^2 error	P_2	H^1 error	P_2
d/2	1.055e-01	Rate	8.156e-01	Rate	2.488e-02	Rate	4.146e-01	Rate
d/4	2.739e-02	1.95	4.027e-01	1.02	3.845e-03	2.69	1.141e-01	1.86
d/8	6.755e-03	2.02	1.955e-01	1.04	5.574e-04	2.79	3.108e-02	1.88
d/16	1.675e-03	2.01	9.587e-02	1.03	7.509e-05	2.89	8.138e-03	1.93
d/32	4.177e-04	2.00	4.763e-02	1.01	9.727e-06	2.95	2.080e-03	1.97

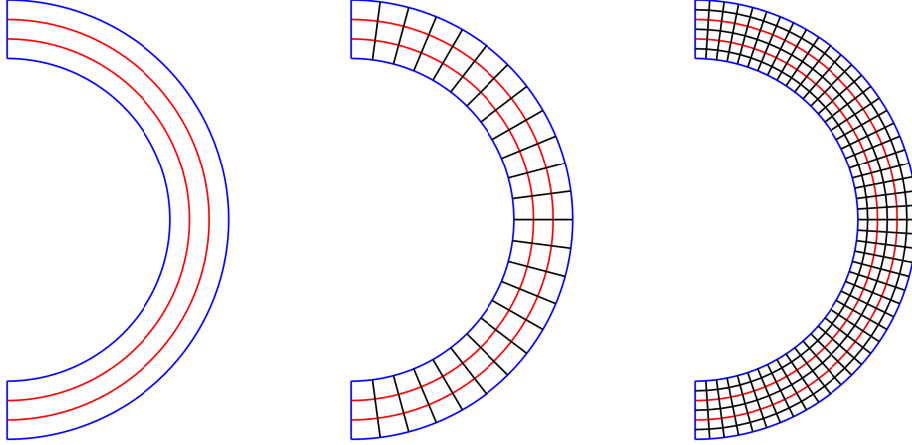


Figure 11: Example 5.2.2. Left: domain; Middle: initial mesh; Right: refined mesh

Table 8: Example 5.2.2. Convergence Rates for P_1 and P_2 Elements, $d \approx 0.42$

$h \approx$	L^2 error	P_1	H^1 error	P_1	L^2 error	P_2	H^1 error	P_2
d/2	5.072e-02	Rate	4.716e-01	Rate	6.251e-03	Rate	1.773e-01	Rate
d/4	1.297e-02	1.97	2.251e-01	1.07	8.378e-04	2.90	4.620e-02	1.94
d/8	3.248e-03	2.00	1.094e-01	1.04	1.093e-04	2.94	1.187e-02	1.96
d/16	8.119e-04	2.00	5.416e-02	1.01	1.395e-05	2.97	3.008e-03	1.98
d/32	2.030e-04	2.00	2.700e-02	1.00	1.761e-06	2.99	7.567e-04	1.99

6. Conclusions

This paper tries to answer the question of solving second-order PDEs on domains with curved Lipschitz continuous boundaries or interfaces by high-order methods if the exact solutions are smooth enough. Our method has arbitrary high order, doesn't introduce geometrical errors, and guarantees optimal convergence rates. Also, basis functions are easy to construct, don't depend on the smoothness of sides/faces, and are consistent in 2D and 3D. Though not given here, the weak Galerkin schemes, for Poisson's equation with Neumann boundary condition or the elliptic interface problem with non-homogeneous jump condition (same as in [11]) also have optimal convergence rates and can be proved similarly. There is still room to improve the current method by reducing the unknowns on the sides/faces as in [29], and it provides a way to deal with small edges/faces in the mesh by combining them and treat the connected lines/faces as a whole side/face. Our next steps are to extend the work to PDEs with nonlinear boundary conditions on curved boundaries or interfaces, which are common in biological models, see [30], and design similar basis functions on curved sides/faces for fourth-order problems.

Acknowledgments

The second author is funded by Grant R01EB034143. The third author has received support from the National Natural Science Foundation of China (Grant Number: 12001325).

References

- [1] G. Guyomarc'h, C.-O. Lee, K. Jeon, A discontinuous galerkin method for elliptic interface problems with application to electroporation, *Communications in numerical methods in engineering* 25 (10) (2009) 991–1008.
- [2] R. Guo, T. Lin, An immersed finite element method for elliptic interface problems in three dimensions, *Journal of Computational Physics* 414 (2020) 109478.
- [3] R. Guo, X. Zhang, Solving three-dimensional interface problems with immersed finite elements: A-priori error analysis, *Journal of Computational Physics* 441 (2021) 110445.
- [4] B. Cockburn, W. Qiu, M. Solano, A priori error analysis for HDG methods using extensions from subdomains to achieve boundary conformity, *Mathematics of computation* 83 (286) (2014) 665–699.
- [5] C. He, S. Zhang, X. Zhang, Error analysis of petrov-galerkin immersed finite element methods, *Computer Methods in Applied Mechanics and Engineering* 404 (2023) 115744.
- [6] J. A. Cottrell, T. J. Hughes, Y. Bazilevs, *Isogeometric analysis: toward integration of CAD and FEA*, John Wiley & Sons, 2009.
- [7] L. Beirão da Veiga, A. Russo, G. Vacca, The virtual element method with curved edges, *ESAIM: Mathematical Modelling and Numerical Analysis* 53 (2) (2019) 375–404.
- [8] J. Wang, X. Ye, A weak Galerkin finite element method for second-order elliptic problems, *Journal of Computational and Applied Mathematics* 241 (2013) 103–115.
- [9] J. Wang, X. Ye, A weak Galerkin mixed finite element method for second order elliptic problems, *Mathematics of Computation* 83 (289) (2014) 2101–2126.
- [10] L. MU, J. WANG, X. YE, Weak Galerkin finite element methods on polytopal meshes., *International Journal of Numerical Analysis & Modeling* 12 (1) (2015) 31–53.
- [11] L. Mu, J. Wang, X. Ye, S. Zhao, A new weak Galerkin finite element method for elliptic interface problems, *Journal of Computational Physics* 325 (2016) 157–173.
- [12] B. Cockburn, J. Gopalakrishnan, F.-J. Sayas, A projection-based error analysis of HDG methods, *Mathematics of Computation* 79 (271) (2010) 1351–1367.
- [13] B. A. de Dios, K. Lipnikov, G. Manzini, The nonconforming virtual element method, *ESAIM: Mathematical Modelling and Numerical Analysis* 50 (3) (2016) 879–904.
- [14] A. Dedner, A. Hodson, Robust nonconforming virtual element methods for general fourth-order problems with varying coefficients, *IMA Journal of Numerical Analysis* 42 (2) (2022) 1364–1399.
- [15] M. Solano, F. Vargas, A high order HDG method for stokes flow in curved domains, *Journal of Scientific Computing* 79 (3) (2019) 1505–1533.
- [16] E. Burman, G. Delay, A. Ern, The unfitted HHO method for the stokes problem on curved domains, in: *Numerical Mathematics and Advanced Applications ENUMATH 2019*, Springer, 2021, pp. 389–397.
- [17] L. Mu, Weak Galerkin finite element with curved edges, *Journal of Computational and Applied Mathematics* 381 (2021) 113038.
- [18] Q. Guan, M. Gunzburger, W. Zhao, Weak-Galerkin finite element methods for a second-order elliptic variational inequality, *Computer Methods in Applied Mechanics and Engineering* 337 (2018) 677–688.

- [19] Q. Guan, Weak Galerkin finite element method for poisson’s equation on polytopal meshes with small edges or faces, *Journal of Computational and Applied Mathematics* 368 (2020) 112584.
- [20] S. Bertoluzza, M. Pennacchio, D. Prada, Weakly imposed dirichlet boundary conditions for 2d and 3d virtual elements, *Computer Methods in Applied Mechanics and Engineering* 400 (2022) 115454.
- [21] Q. Guan, Weak Galerkin finite element method for second order problems on curvilinear polytopal meshes with lipschitz continuous edges or faces, arXiv:1902.02400v1.
- [22] L. Beirão da Veiga, F. Brezzi, L. Marini, A. Russo, Polynomial preserving virtual elements with curved edges, *Mathematical Models and Methods in Applied Sciences* 30 (08) (2020) 1555–1590.
- [23] D. Li, C. Wang, J. Wang, Curved elements in weak Galerkin finite element methods, arXiv preprint arXiv:2210.16907.
- [24] L. Yang, H. Peng, Q. Zhai, R. Zhang, The weak Galerkin finite element method for stokes interface problems with curved interface, arXiv preprint arXiv:2211.11926.
- [25] L. Yemm, A new approach to handle curved meshes in the Hybrid High-Order method, arXiv preprint arXiv:2212.05474.
- [26] S. C. Brenner, L.-Y. Sung, Virtual element methods on meshes with small edges or faces, *Mathematical Models and Methods in Applied Sciences* 28 (07) (2018) 1291–1336.
- [27] J. H. Bramble, S. Hilbert, Estimation of linear functionals on Sobolev spaces with application to Fourier transforms and spline interpolation, *SIAM Journal on Numerical Analysis* 7 (1) (1970) 112–124.
- [28] C. Talischi, G. H. Paulino, A. Pereira, I. F. Menezes, PolyMesher: a general-purpose mesh generator for polygonal elements written in Matlab, *Structural and Multidisciplinary Optimization* 45 (3) (2012) 309–328.
- [29] L. Mu, J. Wang, X. Ye, A weak Galerkin finite element method with polynomial reduction, *Journal of Computational and Applied Mathematics* 285 (2015) 45–58.
- [30] Q. Guan, G. Queisser, Modeling calcium dynamics in neurons with endoplasmic reticulum: Existence, uniqueness and an implicit–explicit finite element scheme, *Communications in Nonlinear Science and Numerical Simulation* 109 (2022) 106354.